Seismic data interpolation using generalised velocity-dependent seislet transform[a]

[a]Published in Geophysical Prospecting, 65, S1, 82-93, (2017)

Yang Liu, Peng Zhang*, Cai Liu**

ABSTRACT

Data interpolation is an important step for seismic data analysis because many processing tasks, such as multiple attenuation and migration, are based on regularly sampled seismic data. Failed interpolations may introduce artifacts and eventually lead to inaccurate final processing results. In this paper, we generalize seismic data interpolation as a basis pursuit problem and propose an iteration framework for recovering missing data. The method is based on nonlinear iteration and sparse transform. A modified Bregman iteration is used for solving the constrained minimization problem based on compressed sensing. The new iterative strategy guarantees fast convergence by using a fixed threshold value. We also propose a generalized velocity-dependent (VD) formulation of the seislet transform as an effective sparse transform, in which the nonhyperbolic normal moveout equation serves as a bridge between local slope patterns and moveout parameters in the common-midpoint domain. It can also be reduced to the traditional VD-seislet if special heterogeneity parameter is selected. The generalized VD-seislet transform predicts prestack reflection data in offset coordinates, which provides a high compression of reflection events. The method was applied to synthetic and field data examples and the results show that the generalized VD-seislet transform can reconstruct missing data with the help of the modified Bregman iteration even for nonhyperbolic reflections under complex conditions, such as VTI media or aliasing.

INTRODUCTION

In an ideal data acquisition system, continuous receivers are set up and each receiver has continuous sources, however, such an ideal system has not been achieved in practice. There are various geometries, and uniform data coverage is rarely achieved because of practical and economic constraints (Stone, 1994). Furthermore, regular data distribution is prerequisite in some applications of seismic migrations (Claerbout, 1971; Gardner and Canning, 1994; Biondi and Palacharla, 1996; Zhang et al., 2003), multiple elimination (Verschuur et al., 1992; Dragoset and Jericevic, 1998), and 4D seismic monitoring (Morice et al., 2000). Under such circumstances, new data points are constructed with known data points through data interpolation. Therefore, data interpolation has become a key technique for data processing in seismic exploration, especially wide azimuth seismic surveys.

Many seismic data interpolation methods have been proposed in the past few years, among which the binning method and its improvements are the simplest. However, they always create artifacts, which affect the final processing results. Another approach is based on different types of continuation operators (Stolt, 2002; Fomel, 2003; Liu and Fomel, 2010). Sometimes, these operators do not give good results at small offset distances because of limited integration apertures. In some methods, data interpolation is applied as an iterative optimization problem using a prediction-error filter (PEF). Several different prediction methods have been proposed, including f-x prediction filter interpolation (Spitz, 1991; Porsani, 1999; Wang, 2002; Naghizadeh and Sacchi, 2009) and t-x domain PEF interpolation (Claerbout and Nichols, 1991; Fomel, 2002; Curry, 2003; Liu and Fomel, 2011). Gülünay (2003) used nonaliased lower frequencies to remove aliases. In fact, Gülünay's method is equivalent to implementing Spitz's method in a different domain. Abma and Kabir (2006b) compared different t-x, f-x, and f-k methods and determined their characteristics. Many interpolation algorithms have been implemented for various scenarios yielding improvements in seismic images. The latest data interpolation technologies bring revolutionary changes in the acquisition design, significantly reducing the cost, and turnaround time for seismic acquisition. Nevertheless, accurate handling of highly aliased seismic data with strongly irregular sampled acquisition grids and handling complex data in which seismic events interfere each other with different amplitudes and noise levels remain challenges for seismic data interpolation algorithms.

If seismic data show sparsity in some domains, compressed sensing (CS) (Donoho, 2006) can be used for reconstructing missing data. CS-based methods for data interpolation usually consist of two parts, namely, sparse transform and iterative algorithm, and recently, they have been undergoing rapid development. There are different iterative approaches to solve the inverse problem corresponding to data interpolation. For instance, Abma and Kabir (2006a) introduced a projection onto convex sets (POCS) algorithm to seismic data interpolation. Liang et al. (2014) proposed a split inexact Uzawa algorithm. Yu et al. (2015) used a two-stage method to solve objective function for data interpolation. Chen et al. (2015) proposed a nonlinear shaping regularization for solving the inverse problem. Different iterative strategies have been designed to control the balance between fast convergence and accurate recovery of missing data. A widely used sparse transform for seismic data interpolation is Fourier transform under plane waves assumption (Xu et al., 2005; Zwartjes and Gisolf, 2007; Zwartjes and Sacchi, 2007; Naghizadeh and Innanen, 2013). The wavelet transform is powerful in representing piecewise signals (Mallat, 2009); however, it is still not suitable for compressing nonstationary seismic data.

Wavelet-like transforms have different applications in seismic data analysis (Herrmann et al., 2008; Wang et al., 2015; Boßmann and Ma, 2015). Seislet transform (Fomel, 2006) is a sparse transform specifically designed for characterizing seismic data. Fomel and Liu (2010) further improved the seislet framework and proposed additional applications. The original seislet transform utilizes local data slopes estimated by plane-wave destruction (PWD) filters (Fomel, 2002; Chen et al., 2013a,b). However, a PWD operator can be sensitive to strong interference, which leads to occasional failure of the PWD-seislet transform in describing noisy signals. To address this problem, Liu et al. (2015) proposed a velocity-dependent (VD) concept where local slopes in prestack data are evaluated from moveout parameters estimated by conventional velocity-analysis techniques.

In this paper, we extended the velocity-dependent (VD)-seislet transform (Liu et al., 2015) to a nonhyperbolic pattern and applied it to data interpolation with a new modified Bregman iteration. We tested the performance of generalized VD-seislet transforms using numerical experiments with synthetic and field data, and the results are described in this paper.

THEORY

Generalized velocity-dependent seislet transform

The seislet framework was defined by Fomel and Liu (2010). It is based on the discrete wavelet transform and different data patterns, such as slopes or frequencies. In plane-wave construction (Fomel and Guitton, 2006; Fomel, 2010), a seismic trace is predicted from its neighbors by following locally varying slopes of seismic events. It has been used for designing PWD-seislet transforms. Liu et al. (2015) proposed a velocity-dependent (VD) slope as the pattern in VD-seislet transform, where the normal moveout (NMO) equation serves as a bridge between local slopes and scanned NMO velocities. Seislet transforms with slope patterns show different characteristics compared to wavelet transform. Wavelet transforms involve no special pattern and sample shift is treated as an elementary prediction. Compared with PWD-seislet transform that predicts local plane waves, VD-seislet transforms involve the traces in common-midpoint (CMP) gather and predict elements along a time-distance curve.

The general guidelines of the lifting scheme (Sweldens and Schröder, 1996) can be followed for the discrete wavelet transform to define seislet transforms. The basic prediction $\mathbf{P}$ and update $\mathbf{U}$ operators for a simple seislet transform are shown as follows (Fomel and Liu, 2010):

$$\mathbf{P}[\mathbf{e}]_k = \left(\mathbf{R}_k^{(+)}[\mathbf{e}_{k-1}] + \mathbf{R}_k^{(-)}[\mathbf{e}_k]\right)/2 \tag{1}$$

$$\mathbf{U}[\mathbf{r}]_k = \left(\mathbf{R}_k^{(+)}[\mathbf{r}_{k-1}] + \mathbf{R}_k^{(-)}[\mathbf{r}_k]\right)/4\ , \tag{2}$$

where $\mathbf{e}_k$ is the even components of data at the k-th transform scale, $\mathbf{r}_k$ is the residual difference between the odd component of data and its prediction from the even component at the k-th transform scale. $\mathbf{R}_k^{(+)}$ and $\mathbf{R}_k^{(-)}$ are operators that predict a component from its left and right neighbors according to different patterns. Equations 1 and 2 are defined by modifying Cohen-Daubechies-Feauveau (CDF) 5/3 biorthogonal wavelet construction (Cohen et al., 1992). A higher-order seislet transform can also be defined by applying biorthogonal wavelets twice with different lifting operator coefficients (Lian et al., 2001). For different types of slope-based seislets, the corresponding operator $\mathbf{R}_k$, which is related to different slope patterns by plane-wave construction (Fomel, 2010), must be defined.

Liu et al. (2015) used the classical hyperbolic model of reflection moveout at near offset to define seismic local slopes

$$t(x) = \sqrt{t_0^2 + \frac{x^2}{v_{rms}^2(t_0)}} \, , \tag{3}$$

where t_0 is the zero-offset traveltime, $t(x)$ is the corresponding traveltime recorded at offset x, and $v_{rms}(t_0)$ is the stacking or root mean square (RMS) velocity obtained through a standard velocity scan.

For more general cases, the shifted hyperbola NMO equation (Malovichko, 1978; Castle, 1994; Fomel and Grechka, 2001) can be used to obtain more accurate slopes in some situations, such as large-offset gather or VTI media. The nonhyperbolic NMO equation is shown as follows:

$$t(x) = t_0(1 - \frac{1}{S}) + \frac{1}{S}\sqrt{t_0^2 + \frac{S\,x^2}{v_{rms}^2(t_0)}} \, , \tag{4}$$

where S is the parameter describing heterogeneity. Equation 4 is reduced to equation 3 when $S = 1$.

The generalized velocity-dependent (VD) slopes $\sigma = dt/dx$ can be calculated by:

$$\sigma(t,x) = \frac{x}{[S(t(x) - t_0) + t_0]v_{rms}^2(t_0, x)} \, . \tag{5}$$

After the generalized velocity-dependent (VD)-slope pattern of seismic data is calculated, pattern-based operators $\mathbf{R}_k$ can be designed through plane-wave construction, which guarantees representation of nonhyperbolic primaries by the generalized VD-seislet transform. When the generalized VD-seislet transform is applied to a CMP gather, the predictable reflection information is compressed to large coefficients at small scales. The sparse characteristic of the generalized VD-seislet transform is suitable for reconstructing missing data in the inverse problem framework.

Modified Bregman iteration for data interpolation

Data reconstruction can be treated as a linear-estimation problem and solved by an iterative optimization algorithm (Fomel, 2003). Let $\mathbf{d}$ be the vector of observed data and $\mathbf{\Phi}$ be the regularized model, one can obtain the model-space regularization equation by using a *forward modeling operator* $\mathbf{L}$:

$$\mathbf{d} = \mathbf{L}\mathbf{\Phi} \; . \tag{6}$$

Missing data interpolation is a particular case of data reconstruction, where the input data are already given on a regular grid. One needs to reconstruct only the missing values in the empty bins. In general, $\mathbf{L}$ is selected as a mask operator $\mathbf{K}$ (a diagonal matrix with zeros at locations of missing data and ones elsewhere), and the problem becomes underdetermined. As an alternative theory of Nyquist/Shannon sampling theory, compressed sensing (CS) provides an important theoretical basis for reconstructing images (Donoho, 2006). Analogous to CS, missing data interpolation can be generalized to a NP-hard problem (Amaldi and Kann, 1998) by using inverse generalized velocity-dependent (VD)-seislet transform $\mathbf{T}$:

$$\min_{\mathbf{m}} \|\mathbf{m}\|_0 \; s.t. \; \mathbf{K}\mathbf{T}\mathbf{m} = \mathbf{d} \; , \tag{7}$$

where $\mathbf{m}$ is the transform coefficient and $\mathbf{\Phi} = \mathbf{T}\mathbf{m}$. Basis pursuit is a traditional method for solving the NP-hard problem (Equation 7), where the corresponding constrained minimization problem is as follows:

$$\min_{\mathbf{m}} \|\mathbf{m}\|_1 \; s.t. \; \mathbf{K}\mathbf{T}\mathbf{m} = \mathbf{d} \; . \tag{8}$$

Equation 8 is a convex optimization problem, which can be transformed into a linear program and then solved by conventional linear programming solvers. Bregman iteration was introduced by Osher et al. (2005) in the context of image processing. This iteration solves a sequence of convex problems (Yin et al., 2008), and its general formulation is as follows:

$$\mathbf{d}^{k+1} = \mathbf{d} + (\mathbf{d}^k - \mathbf{K}\mathbf{T}\mathbf{m}^k) \; , \tag{9}$$

$$\mathbf{m}^{k+1} = \arg\min_{\mathbf{m}} \mu \|\mathbf{m}\|_1 + \frac{1}{2}\|\mathbf{K}\mathbf{T}\mathbf{m} - \mathbf{d}^{k+1}\|_2^2 \; . \tag{10}$$

The advantage of the Bregman iteration is that the penalty parameter μ in equation 10 remains constant. We can therefore choose a fixed value for μ that minimizes the condition number of the sub-problems, which results in a fast convergence.

An iterative procedure based on shrinkage, also called soft thresholding, is used by many researchers to solve equation 10 (Daubechies et al., 2004). However, it is difficult to find the adjoint of $\mathbf{KT}$. In a general case, forward generalized velocity-dependent (VD)-seislet transform $\mathbf{T^{-1}}$ is an approximate inverse of $\mathbf{KT}$; then the chain $\mathbf{T^{-1}KT}$ is close to the identity operator $\mathbf{I}$. Therefore, we can obtain an iteration with shaping regularization (Fomel, 2008) as follows:

$$\mathbf{m}^{k+1} = \mathbf{S}[\mathbf{T^{-1}}\mathbf{d}^{k+1} + (\mathbf{I} - \mathbf{T^{-1}}\mathbf{K}\mathbf{T})\mathbf{m}^k] \; , \tag{11}$$

where $\mathbf{S}$ is soft thresholding. The iteration (equation 11) will converge to the solution of the least-squares optimization problem regularized by a sparsity constraint (equation 10). Equation 11 can be further reformulated as

$$\mathbf{m}^{k+1} = \mathbf{S}[\mathbf{T^{-1}}(\mathbf{d}^{k+1} + (\mathbf{I} - \mathbf{K})\mathbf{T}\mathbf{m}^k)] \; . \tag{12}$$

Combining equation 9 with the shaping solver (equation 12), the framework of modified Bregman iteration is as follows:

$$\begin{aligned} \mathbf{d}^{k+1} &= \mathbf{d} + (\mathbf{d}^k - \mathbf{K}\mathbf{T}\mathbf{m}^k) \; , & (13) \\ \mathbf{m}^{k+1} &= \mathbf{S}[\mathbf{T^{-1}}(\mathbf{d}^{k+1} + (\mathbf{I} - \mathbf{K})\mathbf{T}\mathbf{m}^k)] \; . & (14) \end{aligned}$$

This is the analog of “adding back the residual” in the Rudin-Osher-Fatemi (ROF) model for TV denoising (Osher et al., 2005). By using a large threshold value, the modified Bregman iteration can guarantee fast convergence of the objective function (equation 8) and accurate recovery of the regularized model $\mathbf{\Phi}$. The final interpolated result can be calculated by $\hat{\mathbf{d}} = \mathbf{T}\mathbf{m}^N$, where N is the number of iteration.

SYNTHETIC EXAMPLE

First, we applied the method to a 2D synthetic prestack dataset (Figure 1a), which was created from a 2D slice of the benchmark French model (French, 1974). The reflector with round dome and corners creates reflection events along midpoint and offset axes. The inflection points of the reflector lead to traveltime triplications at some offsets. Then we removed 70% of randomly selected traces (Figure 1b) from the input data (Figure 1a). We directly used NMO equation 3 to analyze data with missing traces because the dataset is limited in a near-offset range. The scanned parameters were obtained and the results are shown in Figure 2a. The velocity spectra of NMO from data show that the picked velocities are reasonable because velocity scan is less sensitive to missing traces. Next, we calculated the velocity-dependent (VD) slopes using the NMO velocities. The VD slopes calculated from equation 5 with $S = 1$ provided accurate results (Figure 2b). Data interpolation with the help of modified Bregman iteration (equations 13 and 14) recovers missing traces as long as seismic data are sufficiently sparse in the transform domain. To demonstrate the superior sparseness of the generalized VD-seislet coefficients, we compare the proposed method with Fourier projection onto convex sets (POCS) interpolation method (Abma and Kabir, 2006a). The results of the interpolation are shown in Figure 3a after carefully selecting parameters. 50 iterations were selected as comparable computational cost as the modified Bregman iteration. Some artificial events were created because Fourier transform cannot provide a naturally sparse domain for curved events. The interpolated error is also slightly large at the locations of the gaps (Figure 4a). The interpolated results can only be partially improved by cutting data into overlapping windows, unless the events display an ideal plane-wave pattern in each window. The generalized VD-seislet transform provides a much sparser domain for reflections. Therefore, the modified Bregman iteration successfully interpolates missing traces (Figure 3b). The number of iteration for the proposed method is 20, which is less than that of Fourier POCS. The difference between the interpolated result and Figure 1a also shows that the proposed method provides reasonable results, in which parts of diffraction events are lost (Figure 4b).

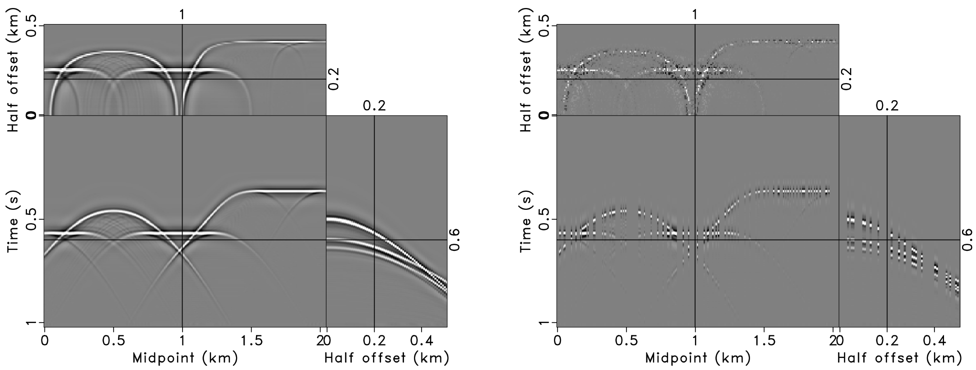

(a) (b)

Figure 1: Synthetic prestack data from the benchmark French model (a) and data with 70% traces removed (b).

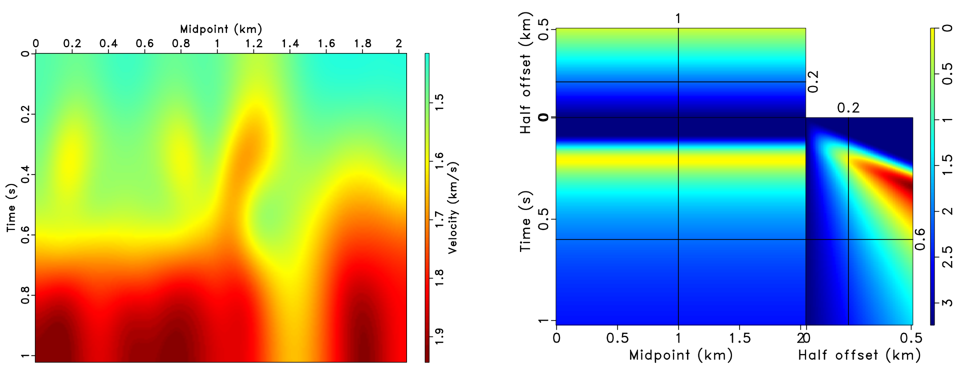

(a) (b)

Figure 2: Velocity spectra by using NMO equation (a) and local slopes calculated by equation 5 with $S = 1$.

The second example is shown in Figure 5a. The amplitudes of the four reflection events show variation because of anisotropy. To evaluate missing trace interpolation (Figure 5b), we removed 70% of randomly selected traces from the input data (Figure 5a). The variation of amplitude and curvature makes it difficult to recover the missing traces. The interpolated results are shown in Figure 6b, which uses the generalized velocity-dependent (VD)-seislet transform and the modified Bregman iteration with 99% percentile-based soft thresholding. The number of iteration is 20. In the interpolated result, it was visually difficult to distinguish the missing trace locations, which indicates successful interpolation. For comparison, we applied the Fourier POCS method to interpolate the missing traces (Figure 6a). The data were

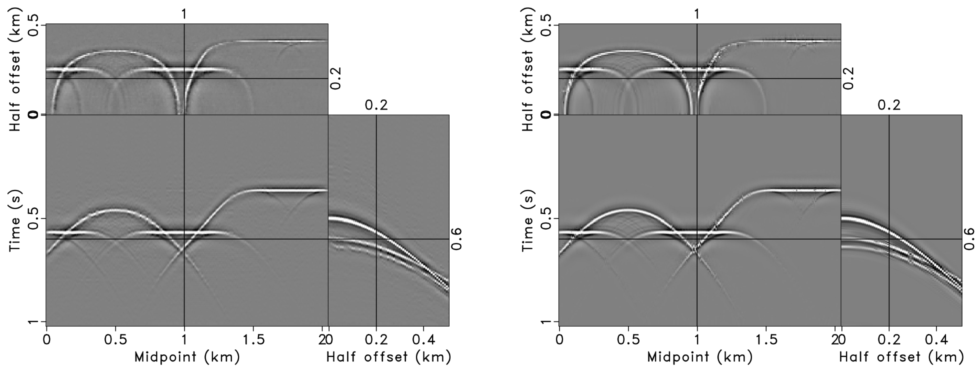

(a) (b)

Figure 3: Interpolated results by using different methods. Fourier POCS method (a) and the proposed method (b).

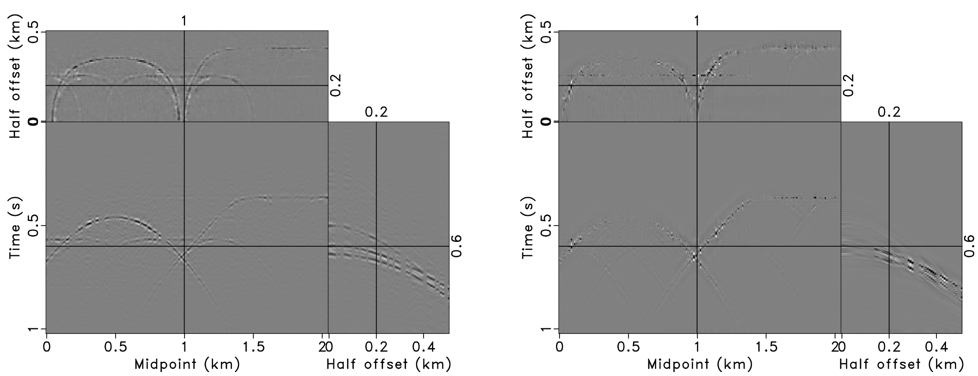

(a) (b)

Figure 4: The difference between interpolated results and synthetic prestack data. Fourier POCS method (a) and the proposed method (b).

divided into seven patches with 43% overlap along the space axis and 200 iterations were run. The POCS method produces a reasonable result after carefully selecting parameters, but some artificial events were still present becausethe uniformed patching windows cannot guarantee the assumption of stationary plane waves.

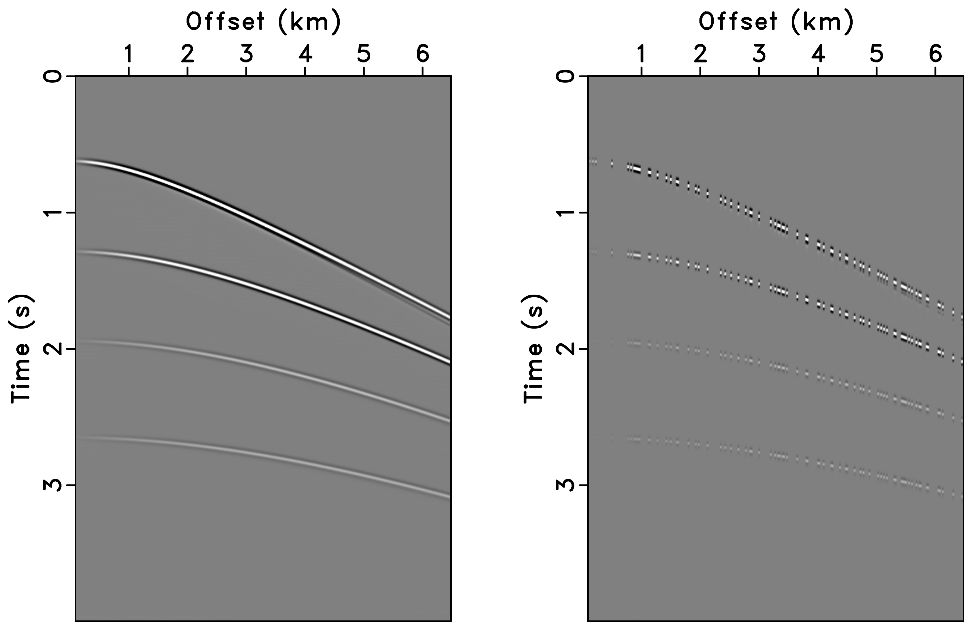

(a) (b)

Figure 5: Synthetic data of VTI media (a) and data with 70% traces removed (b).

FIELD EXAMPLE

To evaluate the performance of the proposed method in field conditions, we used a historic marine dataset from the Gulf of Mexico (Claerbout, 2000). Figure 7a shows the input data, in which near-offset information is completely missing. We removed 40% of randomly selected traces (Figure 7b) from the input data (Figure 7a). The velocity scanning from the missing data can still generate accurate parameter fields using equation 4. Figure 8a and Figure 8b show the velocity spectra and S spectra, respectively. Equation 5 converts RMS velocity and S to seismic pattern (Figure 8c), which displays the varying slopes in CMP gathers and common-offset sections. The generalized velocity-dependent (VD)-seislet transform compresses predictable information according to the local slopes along the offsets. We applied the modified Bregman iteration with the generalized VD-seislet transform to recover missing data. The results show that the missing traces were interpolated well even when anisotropy is present (Figure 9b). For comparison, we applied 3D Fourier transform with POCS (Figure 9a). The Fourier transform could not recover the missing information as accurately as the generalized VD-seislet transform. The results of the 3D Fourier POCS method show obvious gaps caused by inaccurate interpolation, whereas the general-

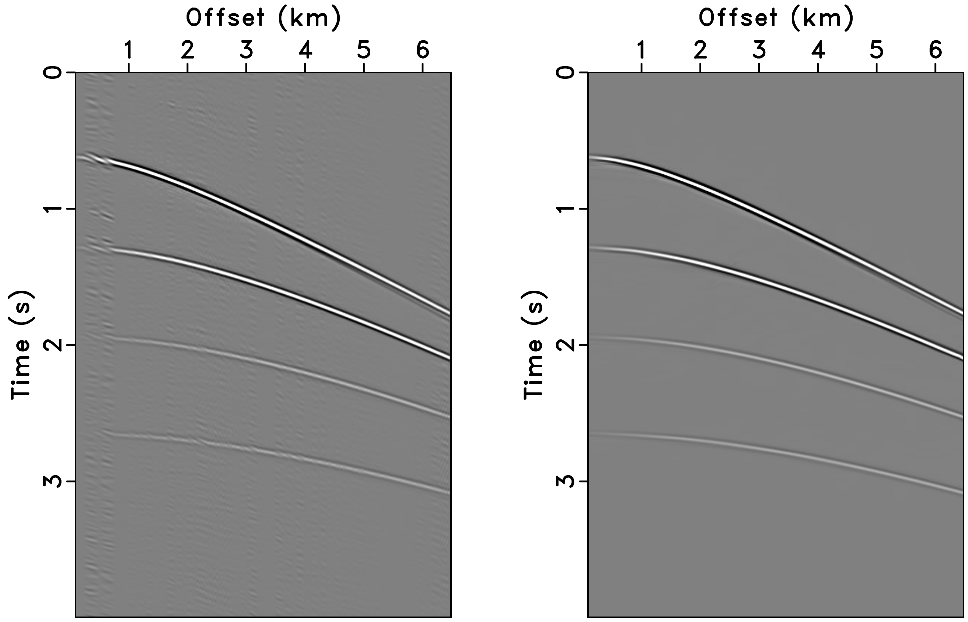

(a) (b)

Figure 6: Interpolated results by using different methods. Fourier POCS method with patching (a) and the proposed method (b).

ized VD-seislet and the modified Bregman iteration strategy provides a reasonably accurate result for interpolating missing data.

If we extend the generalized velocity-dependent (VD)-seislet transform domain along the transform scale axis and recalculate the slope field according to the new x-coordinate axis in equation 5, the inverse generalized VD-seislet transform will accomplish trace interpolation of the input CMP gather (Figure 10a), which is selected from Figure 7a at the midpoint location 11.8925 km. We extended the generalized VD-seislet coefficients with small random noise to consider the existence of realistic noise on different scale levels. Figure 10b shows that the interpolated result provides four times more traces and removes most aliasing. Thus, trace interpolation is a natural operation in the generalized VD-seislet domain.

DISCUSSION

Compared with standard interpolation methods, such as PEF interpolation or Fourier POCS interpolation, the proposed algorithm has different characteristics. First, the generalized velocity-dependent (VD)-seislet transform may have difficulties in handling diffractions, and the velocity scan occasionally produces errors, which would decrease its recovery ability. It is possible to preprocess by using dip moveout. However, the generalized VD-seislet can handle crossing events only up to a certain extent because crossing points only account for a low percentage of data along time-distance

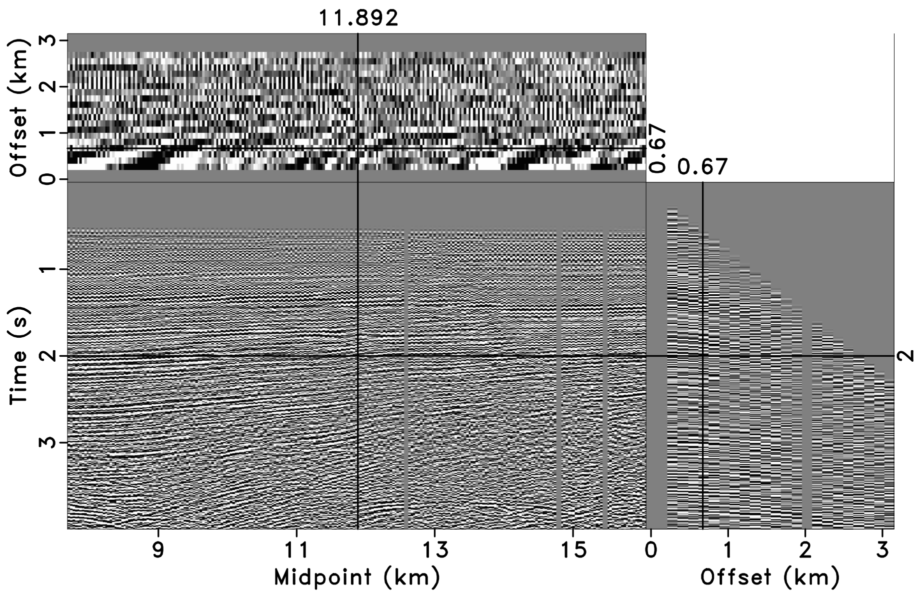

(a)

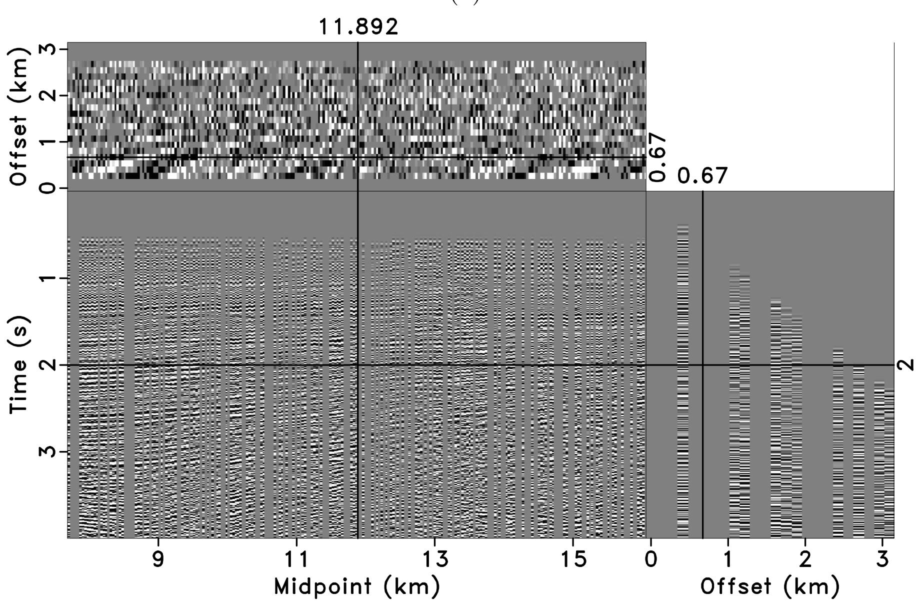

(b)

Figure 7: Marine data with near-offset missing (a) and data with 40% traces removed (b).

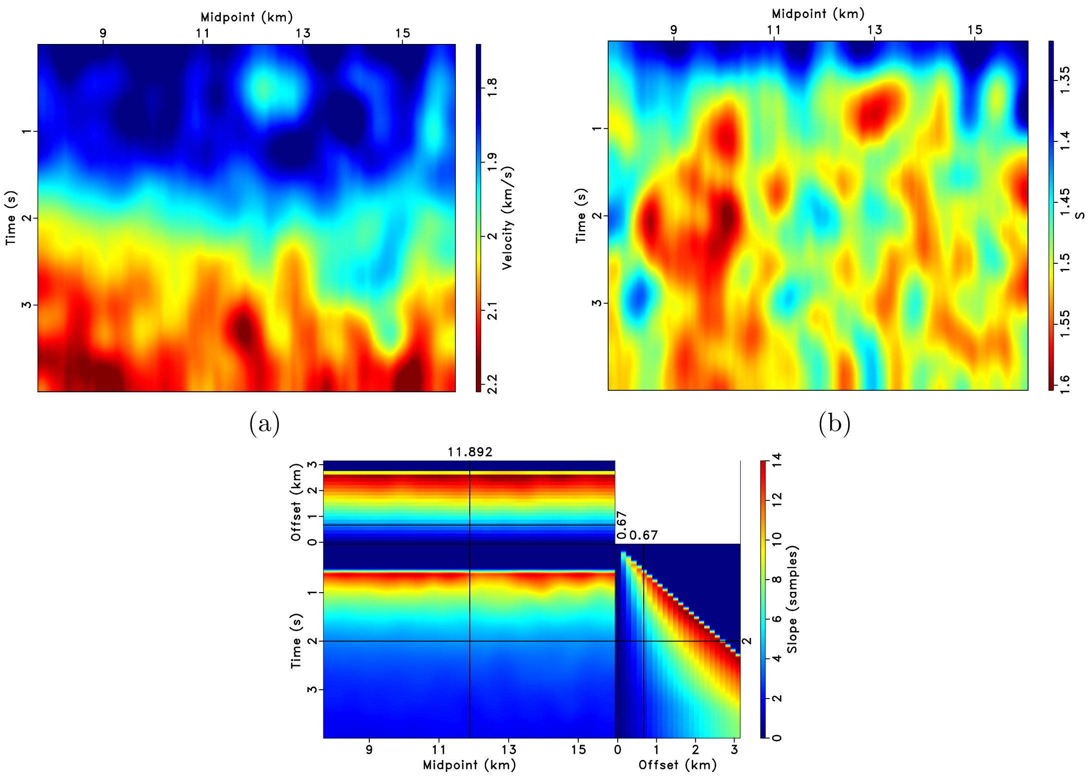

(a) (b) (c)

Figure 8: Velocity section (a) and S section (b) obtained by using equation 4, and velocity-dependent (VD) slopes (c).

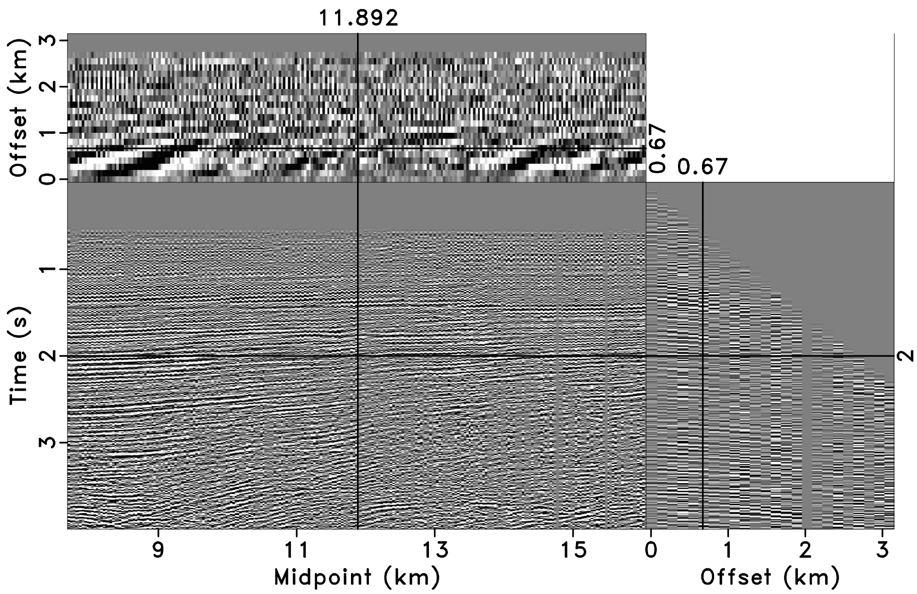

(a)

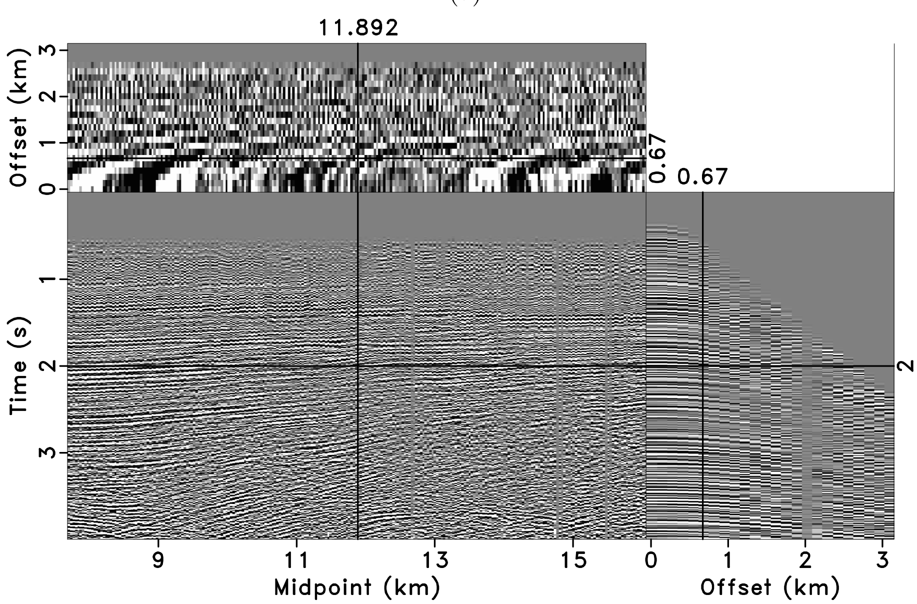

(b)

Figure 9: Interpolated results using different methods. 3D Fourier POCS method (a) and the proposed method (b).

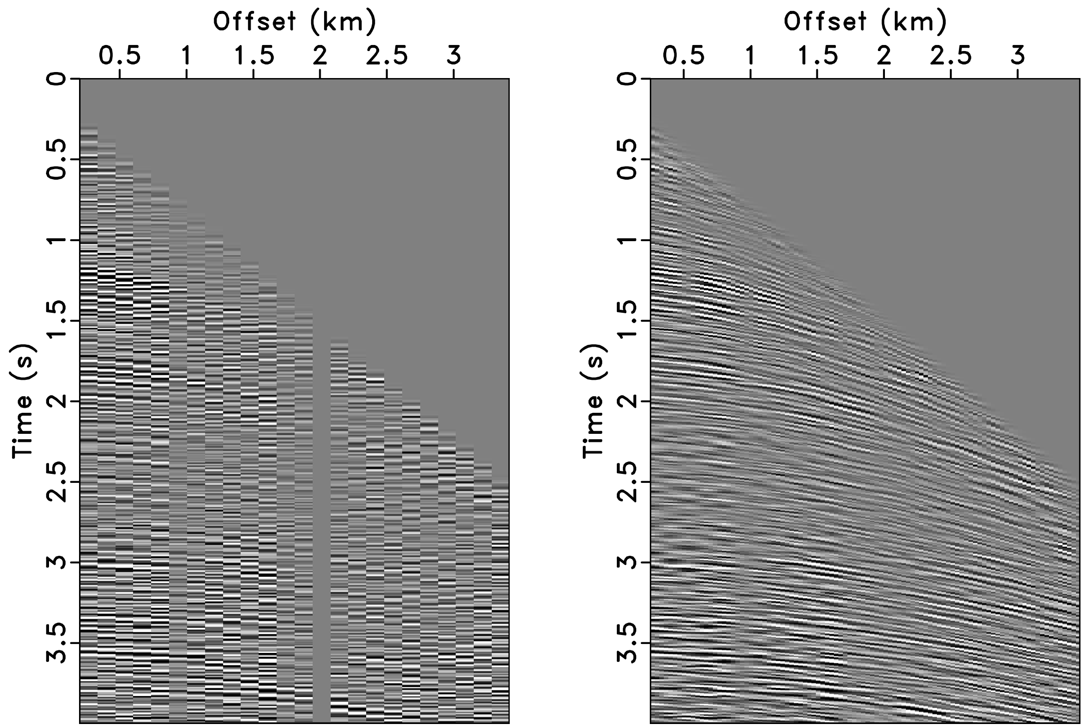

(a) (b)

Figure 10: CMP gather before (a) and after (b) trace interpolation. The interpolated gather has four times more traces than the original one shown in Figure 10a.

curves. It also avoids the problem of event stretch according to the prediction method (Fomel and Liu, 2010), thus producting less artifacts than simple interpolation strategies, such as NMO before data interpolation and subsequent reverting. Meanwhile, standard methods can also not provide accurate interpolation of curved diffractions. Without patching, the generalized VD-seislet transform provides relatively accurate representation of seismic events with aliasing and amplitude anomalies. Fourier POCS are prone to create artifacts, which occur in the frequency-domain method even if data are cut into overlapping windows (patching). Furthermore, data patching causes non-intuitive selection of parameters. The standard PEF interpolation is designed under the assumption of stationary data and becomes less effective when this assumption is violated. Patching in PEF interpolation still fails in the presence of variable dips and usually leads to the problem of insufficient data availability in some child windows, e.g., complete lack of data at near-offset locations and large gaps. Finally, the proposed method applies a modified Bregman iteration, which guarantees fast convergence using a large threshold value, whereas Abma's POCS iteration with linear threshold model produces a slow convergence. Although a different threshold model (Gao et al., 2010) can be used, the POCS method cannot provide fast convergence even with more iterations when random noise are present. Therefore, the proposed method provides an alternative tool for interpolating missing traces in CMP gathers for structurally simple areas even with random noise, amplitude variation, and large gaps.

CONCLUSIONS

In this paper, we introduce a generalized velocity-dependent (VD)-seislet transform, a new domain for analyzing prestack reflection data in the CMP domain. The new transform could compress reflection data away from missing data. The nonhyperbolic NMO equation serves as a bridge between local slopes and scanned parameters that are not sensitive to data gap and aliasing. As examples, we applied the generalized VD-seislet transform in interpolating missing data under the new modified Bregman iteration framework to synthetic and field data. We expect the generalized VD-seislet transform to provide better compression ability for nonhyperbolic reflection events away from interference of missing traces. The current generalized VD-seislet transform based on equation 5 only works for CMP gathers in structurally simple areas. For structurally complex areas, OC-seislet transform (Liu and Fomel, 2010) can perform well but at the expense of high computation cost.

ACKNOWLEDGMENTS

We thank Tijmen Jan Moser, one anonymous associate editor, and two anonymous reviewers for helpful suggestions, which improved the quality of the paper. This work is partly supported by National Natural Science Foundation of China (Grant No. 41522404 and 41430322) and National Key Research and Development Program of

China (Grant No. 2016YFC0600505). All results are reproducible in the Madagascar open-source software environment (Fomel et al., 2013).

REFERENCES

Abma, R., and N. Kabir, 2006a, 3D interpolation of irregular data with a POCS algorithm: Geophysics, **71**, E91–E97.

———, 2006b, Comparisons of interpolation methods in the presence of aliased events: 73rd Annual International Meeting, SEG, Expanded Abstracts, 1909–1912.

Amaldi, E., and V. Kann, 1998, On the approximability of minimizing nonzero variables or unsatisfied relations in linear systems: Theoretical Computer Science, **209**, 237–260.

Biondi, B., and G. Palacharla, 1996, 3D prestack migration of common-azimuth data: Geophysics, **61**, 1822–1832.

Boßmann, F., and J. Ma, 2015, Asymmetric chirplet transform for sparse representation of seismic data: Geophysics, **80**, WD89–WD100.

Castle, R. J., 1994, A theory of normal moveout: Geophysics, **59**, 983–999.

Chen, Y., L. Zhang, and L. Mo, 2015, Seismic data interpolation using nonlinear shaping regularization: Journal of Seismic Exploration, **24**, 327–342.

Chen, Z., S. Fomel, and W. Lu, 2013a, Accelerated plane-wave destruction: Geophysics, **78**, V1–V9.

———, 2013b, Omnidirectional plane-wave destruction: Geophysics, **78**, V171–V179.

Claerbout, J., and D. Nichols, 1991, Interpolation beyond aliasing by (t-s) domain PEFs: 53rd Annual International Meeting, EAGE, Expanded Abstracts, A001.

Claerbout, J. F., 1971, Toward a unified theory of reflector mapping: Geophysics, **36**, 467–481.

———, 2000, Basic Earth imaging: Stanford Exploration Project, `http://sepwww.stanford.edu/sep/prof/`.

Cohen, A., I. Daubechies, and J. Feauveau, 1992, Biorthogonal bases of compactly supported wavelets: Communications on Pure and Applied Mathematics, **45**, 485–560.

Curry, W., 2003, Interpolation sampled data with nonstationary, multiscale prediction-error filters: 73rd Annual International Meeting, SEG, Expanded Abstracts, 1913–1916.

Daubechies, I., M. Defries, and C. D. Mol, 2004, An iterative thresholding algorithm for linear inverse problems with a sparsity constraint: Communications on Pure and Applied Mathematics, **LVII**, 1413–1457.

Donoho, D. L., 2006, Compressed sensing: IEEE Transactions on Information Theory, **52**, 1289–1306.

Dragoset, W. H., and Z. Jericevic, 1998, Some remarks on surface multiple attenuation: Geophysics, **63**, 772–789.

Fomel, S., 2002, Applications of plane-wave destruction filters: Geophysics, **67**, 1946–1960.

———, 2003, Seismic reflection data interpolation with differential offset and shot continuation: Geophysics, **68**, 733–744.

———, 2006, Towards the seislet transform: 76th Annual International Meeting, SEG, Expanded Abstracts, 2847–2851a.

———, 2008, Nonlinear shaping regularization in geophysical inverse problems: 78th Annual International Meeting, SEG, Expanded Abstracts, 2046–2051.

———, 2010, Predictive painting of 3D seismic volumes: Geophysics, **75**, A25–A30.

Fomel, S., and V. Grechka, 2001, Nonhyperbolic reflection moveout of P waves. An overview and comparison of reasons, *in* CWP-372: Colorado School of Mines.

Fomel, S., and A. Guitton, 2006, Regularizing seismic inverse problems by model re-parameterization using plane-wave construction: Geophysics, **71**, A43–A47.

Fomel, S., and Y. Liu, 2010, Seislet transform and seislet frame: Geophysics, **75**, V25–V38.

Fomel, S., P. Sava, I. Vlad, Y. Liu, and V. Bashkardin, 2013, Madagascar: open-source software project for multidimensional data analysis and reproducible computational experiments: Journal of Open Research Software, **1**, e8; doi: https://doi.org/http://dx.doi.org/10.5334/jors.aghttp://dx.doi.org/10.5334/jors.ag.

French, M. S., 1974, Two-dimensional and three-dimensional migration of model-experiment reflection profiles: Geophysics, **39**, 265–277.

Gao, J., X. Chen, J. Li, G. Liu, and J. Ma, 2010, Irregular seismic data reconstruction based on exponential threshold model of POCS method: Applied Geophysics, **7**, 229–238.

Gardner, G. G. F., and A. Canning, 1994, Effects of irregular sampling on 3D prestack migration: 64th Annual International Meeting, SEG, Expanded Abstracts, 1553–1556.

Gülünay, N., 2003, Seismic trace interpolation in the Fourier transform domain: Geophysics, **68**, 355–369.

Herrmann, F., D. Wang, D. Hennenfent, and P. Moghaddam, 2008, Curvelet-based seismic data processing: a multiscale and nonlinear approach: Geophysics, **73**, A1–A5.

Lian, C., K. Chen, H. Chen, and L. Chen, 2001, Lifting based discrete wavelet transform architecture for JPEG2000: The 2001 IEEE International Symposium on Circuits and Systems, IEEE, II445–II448.

Liang, J., J. Ma, and X. Zhang, 2014, Seismic data restoration via data-driven tight frame: Geophysics, **79**, V65–V74.

Liu, Y., and S. Fomel, 2010, OC-seislet: Seislet transform construction with differential offset continuation: Geophysics, **75**, WB235–WB245.

———, 2011, Seismic data interpolation beyond aliasing using regularized nonstationary autoregression: Geophysics, **76**, V69–V77.

Liu, Y., S. Fomel, and C. Liu, 2015, Signal and noise separation in prestack seismic data using velocity-dependent seislet transform: Geophysics, **80**, WD117–WD128.

Mallat, S., 2009, A wavelet tour of signal processing: The sparse way: Academic Press.

Malovichko, A. A., 1978, A new representation of the traveltime curve of reflected waves in horizontally layered media: Applied Geophysics (in Russian), **91**, 47–53, English translation in Sword.sep.51.313.

Morice, S., S. Ronen, P. Canter, K. Welker, and D. Clark, 2000, The impact of positioning differences on 4D repeatability: 70th Annual International Meeting, SEG, Expanded Abstracts, 1611–1614.

Naghizadeh, M., and K. A. Innanen, 2013, Two-dimensional fast generalized Fourier interpolation of seismic records: Geophysical Prospecting, **61**, 62–76.

Naghizadeh, M., and M. Sacchi, 2009, f-x adaptive seismic-trace interpolation: Geophysics, **74**, V9–V16.

Osher, S., M. Burger, D. Goldfarb, J. Xu, and W. Ying, 2005, An iterated regularization method for total variatrion-based image restoration: Multiscale Modeling & Simulation, **4**, 460–489.

Porsani, J. M., 1999, Seismic trace interpolation using half-step prediction filters: Geophysics, **64**, 1461–1467.

Spitz, S., 1991, Seismic trace interpolation in the f-x domain: Geophysics, **56**, 785–794.

Stolt, R. H., 2002, Seismic data mapping and reconstruction: Geophysics, **67**, 890–908.

Stone, D. G., 1994, Designing surveys in two and three dimension: Society of Exploration Geophysicists.

Sweldens, W., and P. Schröder, 1996, Building your own wavelets at home, *in* Wavelets in Computer Graphics: ACM SIGGRAPH Course notes, 15–87.

Verschuur, D. J., A. J. Berkhout, and C. P. A. Wapenaar, 1992, Adaptive surface-related multiple elimination: Geophysics, **57**, 1166–1177.

Wang, X., J. Gao, W. Chen, and C. Yang, 2015, The seismic random noise attenuation method based on enhanced bandelet transform: Journal of Applied Geophysics, **116**, 146–155.

Wang, Y., 2002, Seismic trace interpolation in the f-x-y domain: Geophysics, **67**, 1232–1239.

Xu, S., Y. Zhang, D. Pham, and G. Lambaré, 2005, Antileakage Fourier transform for seismic data regularization: Geophysics, **70**, V87–V95.

Yin, W., S. Osher, D. Goldfarb, and J. Darbon, 2008, Bregman iterative algorithms for l_1 minimization with applications to compressed sensing: SIAM Journal on Imaging Sciences, **1**, 143–168.

Yu, S., J. Ma, X. Zhang, and M. D. Sacchi, 2015, Interpolation and denoising of high-dimensional seismic data: Geophysics, **80**, V119–V132.

Zhang, Y., G. Zhang, and N. Bleistein, 2003, True amplitude wave equation migration arising from true amplitude one-way equations: Inversion Problem, **19**, 1113–1138.

Zwartjes, P., and A. Gisolf, 2007, Fourier reconstruction with sparse inversion: Geophysical Prospecting, **55**, 199–221.

Zwartjes, P., and M. Sacchi, 2007, Fourier reconstruction of nonuniformly sampled, aliased seismic data: Geophysics, **72**, V21–V32.